

# Silicon Photomultipliers for Neutrino Telescopes

Diego Real \* and David Calvo 

IFIC—Instituto de Física Corpuscular, CSIC—Universitat de València, c/Catedrático José Beltrán, 2, 46980 Paterna, Valencia, Spain

\* Correspondence: real@ific.uv.es

**Abstract:** Neutrino astronomy has opened a new window to the extreme Universe, entering into a fruitful era built upon the success of neutrino telescopes, which have already given a new step forward in this novel and growing field by the first observation of steady point-like sources already achieved by IceCube. Neutrino telescopes equipped with Silicon PhotoMultipliers (SiPMs) will significantly increase in number, because of their excellent time resolution and the angular resolution, and will be in better condition to detect more steady sources as well as the unexpected. The use of SiPMs represents a challenge to the acquisition electronics because of the fast signals as well as the high levels of dark noise produced by SiPMs. The acquisition electronics need to include a noise rejection scheme by implementing a coincidence filter between channels. This work discusses the advantages and disadvantages of using SiPMs for the next generation of neutrino telescopes, focusing on the possible developments that could help for their adoption in the near future.

**Keywords:** silicon photomultipliers; neutrino telescopes; time to digital converters; electronics acquisition



**Citation:** Real D.; Calvo, D. Silicon Photomultipliers for Neutrino Telescopes. *Universe* **2023**, *9*, 326. <https://doi.org/10.3390/universe9070326>

Academic Editors: Mihai Horoi, Hiro Ejiri and Andrei Neacsu

Received: 18 June 2023  
Revised: 28 June 2023  
Accepted: 4 July 2023  
Published: 10 July 2023



**Copyright:** © 2023 by the authors. Licensee MDPI, Basel, Switzerland. This article is an open access article distributed under the terms and conditions of the Creative Commons Attribution (CC BY) license (<https://creativecommons.org/licenses/by/4.0/>).

## 1. Introduction

Neutrino astronomy has entered into a new and fruitful era built upon the success of neutrino telescopes. The IceCube Telescope [1] has proven the existence of a diffuse flux of high-energy cosmic neutrinos [2,3], has identified the first high-energy neutrino in correlation with a transient source [4], and not only is demonstrating the first hints of steady sources [5], but has already detected the first neutrinos coming from a steady source, the NCG 1068 [6]. After these discoveries, a rich harvest of new results is rapidly increasing our knowledge of the Universe at high energy. On the other side, the long list of results of ANTARES [7] has shown the feasibility of undersea telescopes, paving the way for its successor, KM3NeT [8], currently under construction, with 36 lines already deployed and taking data. KM3NeT will focus on the search for cosmic neutrino sources in the context of the new multi-messenger era, which can solve one of the oldest mysteries in physics, the origin of high-energy cosmic rays, placing KM3NeT together with IceCube in the frontline of many hot physics topics and clearing the path for new discoveries in the novel and growing [9,10] field of neutrino astronomy.

The improvement in the angular resolution of state-of-the-art neutrino telescopes is critical for the success of pinpointing neutrino steady point-like sources [11]. The use of SiPMs [12–14], either in combination with PhotoMultiplier Tubes (PMTs) or stand-alone, as detector elements in the next generation of telescopes will increase, because of their great time characteristics, the angular resolution [15], and thus the probabilities of detecting steady point-like sources, without forgetting that telescopes with higher resolution also increase the likelihood of detecting the unexpected [16]. SiPMs offer fast responses and low jitter, key factors to increase the angular resolution. Overall, the angular resolution could be significantly increased in water telescopes equipped with SiPMs, which would be an extremely high gain. In ice telescopes, although the angular resolution improvement would not be so remarkable as it is limited by the strong light scattering, it would be

still significant, and, additionally, they could benefit from the manifold advantages of the SiPMs, such as a larger detection area with a higher photon efficiency and higher segmentation, which provides higher angular directivity to the photons arriving. The technological challenge of equipping neutrino telescopes with SiPMs, keeping most of the timing information while mitigating the effects of their intrinsic high dark noise, has prevented their use in neutrino telescopes until now. Another characteristic that can affect the performance of the system is the so-called after pulses. After pulses refer to delayed signals that are generated by SiPMs after detecting an initial photon or light pulse. The presence of after pulses can have significant effects on acquisition systems like the distortion of the time response, causing inaccuracies in the timing measurements. This can lead to errors in determining the arrival time of photons or particles, affecting the overall precision of the system. To mitigate the effects of after pulses, various techniques can be employed. One common approach is to implement suitable signal processing algorithms that can identify and reject after pulses based on their characteristic features; however, mitigating the effect of after pulses is beyond the scope of this article. The present work starts by discussing the detection principle of neutrino telescopes in Section 2 and the state-of-the-art acquisition node for neutrino telescopes in Section 3. The advantages of using SiPMs in neutrino telescopes acquisition nodes are discussed in Section 4, while the challenges for the acquisition electronics are evaluated in Section 5. The possible architectures are discussed in Section 6, and finally, some conclusions are presented in Section 7.

## 2. Neutrino Telescope Detection Principle

Neutrino telescopes are composed of a 3D matrix array of optical sensors deployed in a transparent medium. See Figure 1 for a schematic representation of a neutrino telescope. The detection principle, inspired by an original proposal by Markov [17], is based on the collection of Cherenkov photons produced along the path of relativistic charged particles emerging from neutrino interactions inside or in the vicinity of the telescope. The arrival time of the Cherenkov photons, together with the position of the optical sensors, allows for reconstructing the trajectory of the primary neutrino. The resolution of the reconstructed neutrino trajectory in the detector depends on the accurate measurement of the arrival time of the light on the optical sensors. Neutrino telescope acquisition systems were traditionally based on time to digital converters (TDCs) [18,19], analog to digital converters [20,21], or both [22,23], with acquisition frequencies of about 1 GigaSample Per Second (GSPS). The acquisition resolution of 1 ns is considered enough to maintain the angular resolution determined by the medium properties (ice or water) and the timing properties of the light sensor used, which in all cases was a single PMT housed in a glass sphere.

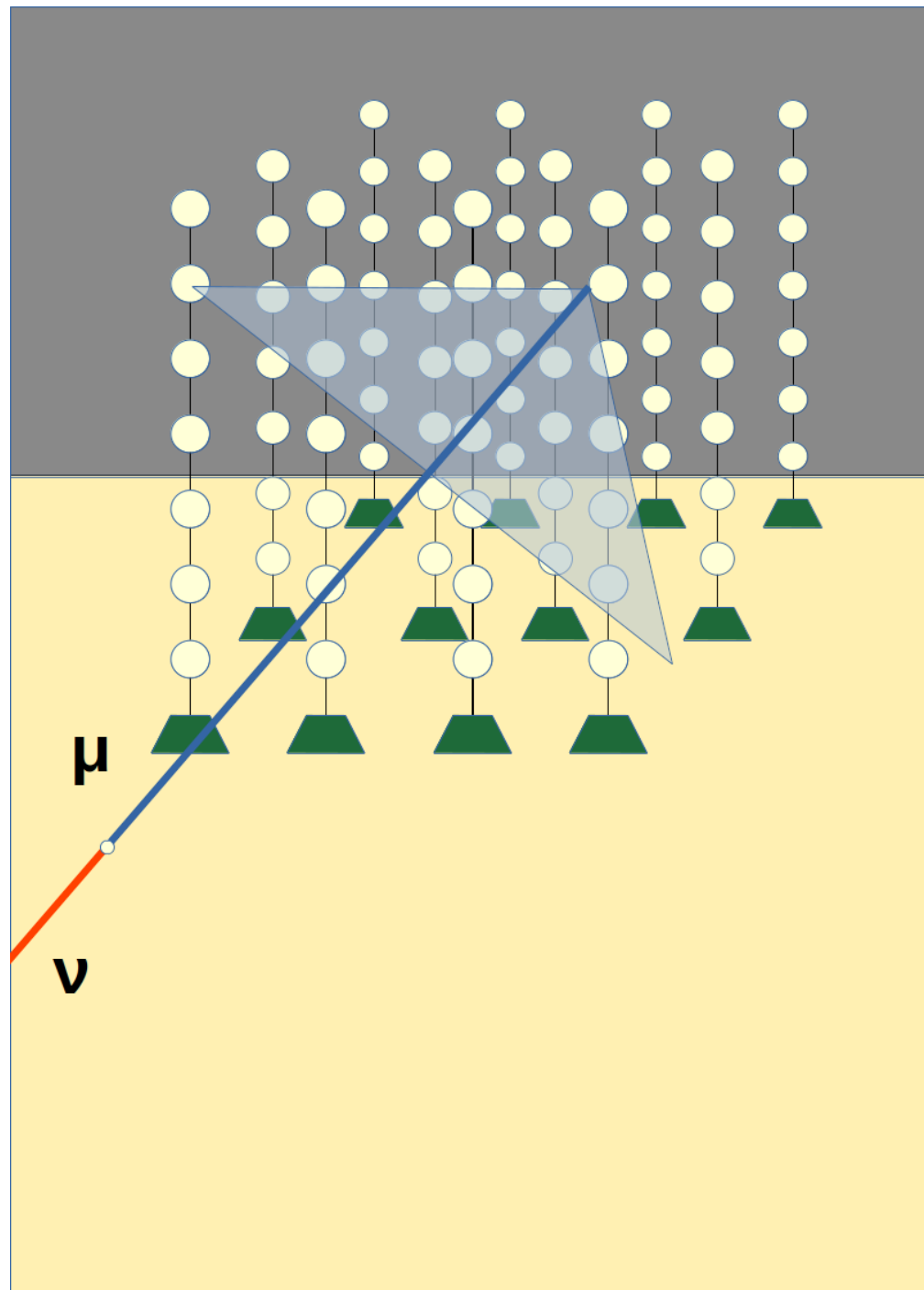


**Figure 1.** Schematic view of a neutrino telescope. The detection of the cherenkov light produced by relativistic particles by the telescope nodes tracks the trajectory of the original neutrino.

### 3. State-of-the-Art Detection Node for Neutrino Astronomy

KM3NeT has made the innovative bet for the multi-PMT Digital Optical Modules (DOMs) [24] with  $4\pi$  coverage obtained by instrumenting  $31 \times 3''$  small PMTs instead of a large photocathode surface PMT. The multi-PMT DOM increases the detection area by multiplying the area of a single and large PMT by three. The DOM also adds sensitivity to the incoming direction of detected photons, which improves the angular resolution. The Multi-PMT DOM improves KM3NeT's angular resolution by around two times that of ANTARES, and around three times that of IceCube [25], which is affected by the strong light scattering of ice. The development of the multi-PMT DOM was possible because the

acquisition system developed maintains the 1 ns resolution in the 31 TDC channels, while the use of resources was kept low to integrate the electronics inside the DOM. The TDCs are embedded in a Field Programmable Gate Array (FPGA), which allows for a remote and safe reconfiguration of the front-end firmware, which adds flexibility to the system. Another innovative approach used by KM3NeT, which has also helped to integrate the acquisition electronics inside the DOM, is the distribution of the synchronisation clock via the communication channels [26,27] instead of using separate synchronisation lines. The integration of the protocol White Rabbit [28–30] at the acquisition node [31,32] allows for a subnanosecond synchronisation level in an integrated manner. An additional improvement achieved is the integration of time calibration instrumentation [33] by miniaturising the ANTARES LED optical beacon [34]. The approach taken for the treatment of the acquired data in the detection nodes was the so-called “all-data-to-shore” strategy [35,36]. By this scheme, all the TDC data are sent to the central station. A computing farm analyses the data by performing different levels of trigger, filtering the data that are not interesting for track reconstructions [37]. Due to its many advantages, the multi-PMT has been proposed for ice detectors, and the upgrade of IceCube [38] will use it [39–41]. At the moment, the multi-PMT DOM is the state-of-the-art detector node [24] for neutrino telescopes, as is its acquisition system [42]. The evolution of optical modules in neutrino telescopes is represented in Figure 2.

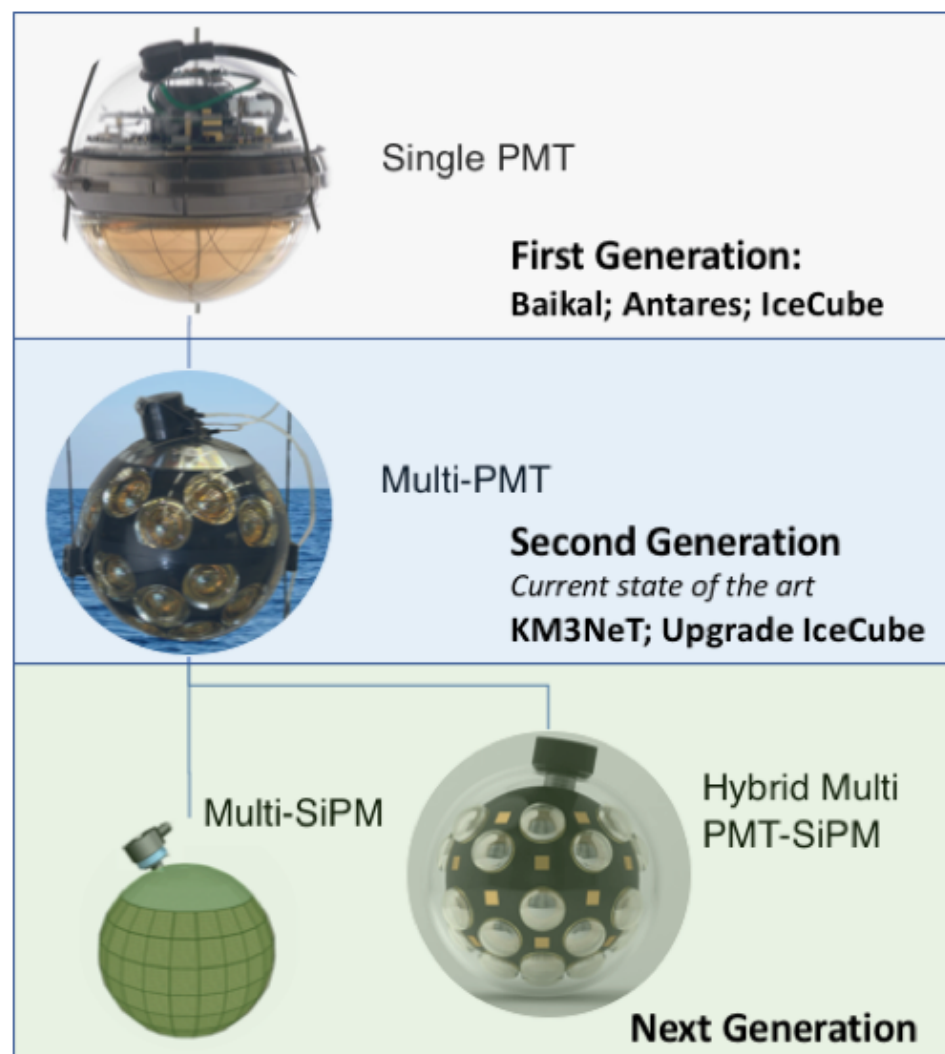


**Figure 2.** Phylogenetic tree of neutrino telescope detection nodes. The Multi-PMT DOM is the state of the art. The next generation of detectors will be based on SiPMs.

#### 4. SiPMs as Detector Elements in Neutrino Telescope DOMs: Advantages and Disadvantages

The use of SiPMs in the acquisition node of neutrino telescopes, either replacing or complementing the PMTs already used, can substantially improve the angular resolution [15] and thus increase the pinpointing capabilities of neutrino telescopes [11]. Their good time resolution, with rise times lower than a quarter of a nanosecond [14,43] and time transit spreads (TTSs) of similar characteristics [14,44,45], make SiPMs an ideal candidate to be used in the next generation of neutrino telescopes, which requires that the acquisition system goes beyond the 1 ns resolution used traditionally in neutrino telescopes [18,19]. SiPMs consist of a Geiger mode avalanche photodiode array on a common silicon substrate [46]. There are typically 1000 microcells (pixels) in a 1 mm<sup>2</sup> area parallelly connected in SiPMs. Each pixel bears a similarity to a photodiode and a quenching resistor in series, which results in a uniform response. Besides the good timing information, SiPMs possess a set of additional characteristics that make them even more appropriate for neutrino telescopes:

- Their sensitivity ranges from ultraviolet to near infrared, ideal for Cherenkov light;
- Unlike PMTs, SiPMs do not require a high voltage supply exceeding 100 V; nonetheless, their gains are comparable to traditional PMTs ( $10^5$ – $10^6$ );
- They are immune to electromagnetic fields;
- The compactness can be scaled up as required and has a relatively lower cost than PMTs [47];
- SiPMs provide excellent single photon resolution [48]. See Figure 3;
- They are stable to temperature variations;
- Benefiting from solid-state technology, SiPMs cannot be damaged by stray light;
- They have a high photon detection efficiency (PDE), with values over 50% in blue [49], while it is 30% in KM3NeT PMTs [50]. See Figure 4;
- In addition, there is a significant number of producers, being a hot sector with an increasing market and associated R&D [51,52].

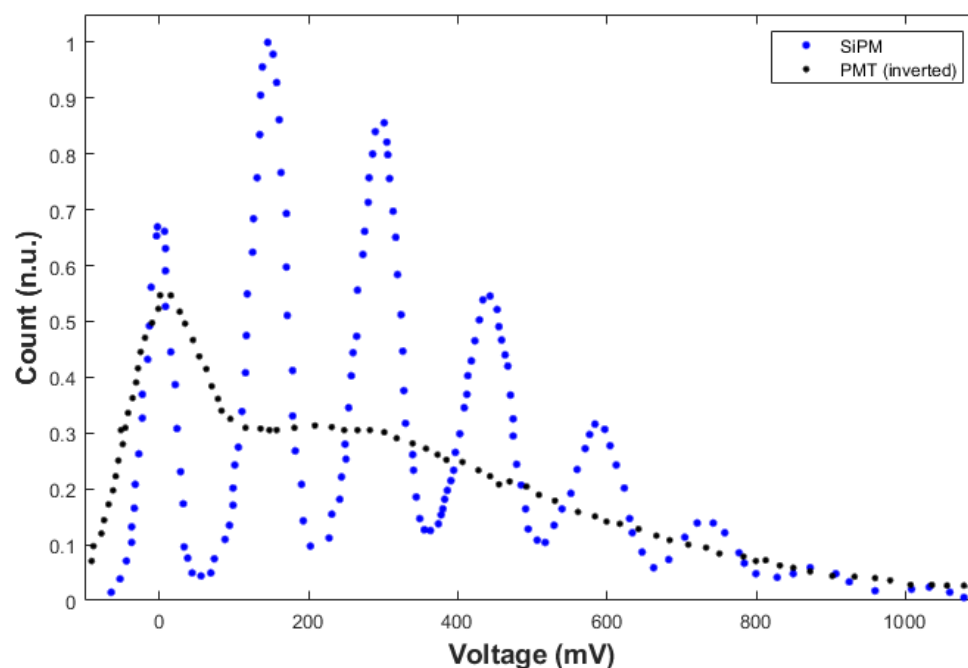


**Figure 3.** Single photon counting pattern for a SiPM and a PMT under the same conditions. The SiPM considerably improves the PMT single photon counting resolution. Plot obtained from [48]. The data have been normalised.

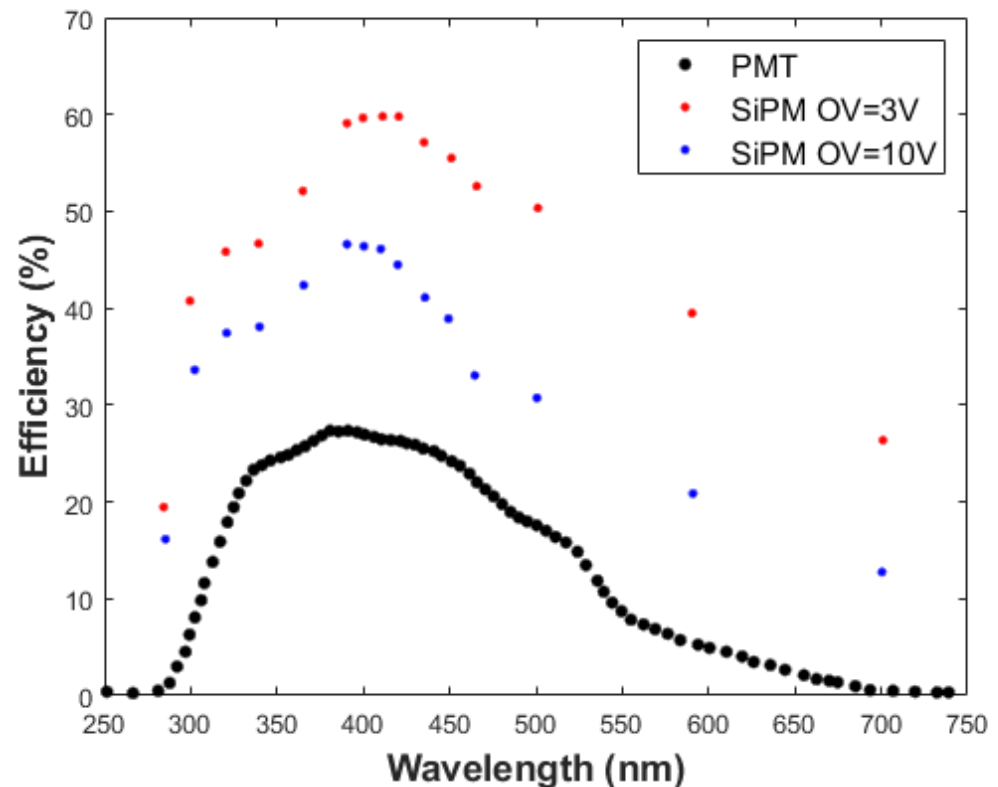


**Figure 4.** Photon detection efficiency of SiPMs with respect the photon wavelength [49] versus PMT quantum efficiency of KM3NeT 3" PMTs (R12199-02) [50].

The characteristics of the SiPMs can increase the efficiency, the detection area, the directional sensitivity, and, overall, the angular resolution. On the other hand, SiPMs present a very high dark count rate (DCR), which cannot be processed by state-of-the-art neutrino telescope acquisition systems. Although DCRs have gone from 1 Mcps/mm<sup>2</sup> to below 40 kcps/mm<sup>2</sup> in recent years, the dark noise is significantly higher than in PMTs and is a challenge for their use in neutrino telescopes. For comparison, PMTs in KM3NeT have an average dark noise of about 0.28 cps/mm<sup>2</sup> [50], so more than five orders of magnitude lower than SiPMs. SiPM DCRs are produced by the thermal generation of carriers, trap-assisted tunnelling, or band gap tunnelling, and the signal produced is equal to a single photon response, and is hence indistinguishable. In addition, the DCR is highly affected by temperature, decreasing the dark noise to half its value every eight degrees [53]. The effect of temperature on the DCR is an important object of study, as is the use of optical accessories to increase the collection efficiency and reduce the DCR. KM3NeT already uses an expansion cone for each PMT, which has achieved an increase of 30% in the collection efficiency [54]. A similar device could be used with SiPMs as well as the use of SiPMs integrated with optical lenses, which would increase the collection area while reducing the DCR [55]. The DCR in state-of-the-art SiPMs is about 20–30 kHz/mm<sup>2</sup> [56–58], which represents, together with the fast timing characteristics, a challenge for the acquisition system which has, so far, prevented their use in neutrino telescopes.

## 5. Challenges Ahead for the Acquisition System

### 5.1. Acquisition Resolution

The extraordinary time resolution of SiPMs, key to increasing the angular resolution of the next generation of neutrino telescopes, requires that the acquisition system has enough resolution. The special operation characteristics of neutrino telescopes and the number of channels involved require a low-resource acquisition architecture as it reduces the

complexity of the acquisition system, increases reliability, and reduces power consumption, very costly to bring to the bottom of the sea or inside an ice block.

The state-of-the-art acquisition resolution for neutrino telescopes is one nanosecond, used to read out PMTs with a TTS of about 5 ns, with a rise time in the same range [50]. SiPM timing characteristics, with rise times lower than a quarter of nanosecond [14,43] and TTSs of similar characteristics [14,44], require an acquisition resolution better than 250 ps to not degrade the timing information [45,59]. Additionally, the use of resources should be kept low, as the acquisition electronics have to be embedded in low-power consumption detection nodes. The development of subnanosecond TDCs seems to be the most reasonable approach. These TDCs should have resolutions below 250 ps, which could be achieved by considerably improving the current TDC architecture. TDCs measure time intervals, detecting the arrival time of the leading edge of a digital pulse and measuring the duration of the pulse [60], and are the main acquisition method used in state-of-the-art neutrino telescopes with the aforementioned one nanosecond resolution. TDCs can be implemented either in application-specific integrated circuits (ASICs) or FPGAs. Although TDCs implemented in ASICs provide better performances, the design process is not only expensive but also complex due to the long turn-around time and layout phase. On the other hand, FPGAs provide a faster development time and the flexibility to adapt the logic to the operation conditions even after the deployment of the detection node. Moreover, it is possible to use the rest of the FPGA resources to process the TDC data and to interface with the rest of the DAQ system, which results in a higher reliability. For all these reasons, TDCs implemented in FPGAs are more appropriate for neutrino telescope acquisition systems than ASICs. The simplest method to implement a TDC using a synchronous system is the counter method. The time interval is calculated by counting the cycles of a reference clock.

In Figure 5, the operation mode of the counter method is shown. In order to increase the resolution, the clock frequency has to be increased, as the resolution is directly proportional to the clock frequency. The main advantage of the counter method is that the range can be increased with the number of bits of the counter. The clock frequency limits the resolution of the TDCs. In FPGAs, the maximum frequency that can be obtained is in the range of 500–660 MHz [61], which implies a maximum resolution of 1.5–2 ns. There are two intervals, one at the beginning of the input pulse and another at the end, where the time information is missing. A different method can be used to measure these intervals with a higher resolution. This combination of methods is called the interpolation or Nutt method [62]. The interpolation method used in state-of-the-art neutrino telescopes is the oversampling technique [63–66], as it is a synchronous method with low resource occupancy. The use of additional clocks with the same frequency but different phases allows for obtaining extra information at the start and end of the pulse. The oversampling method has been implemented using special serialization and deserialization hardware available in the FPGA, which further optimise the use of resources. In total, 32 TDC channels of 1 ns resolution have been developed for their use in the multi-PMT DOM [19,67]. This level of resolution is clearly insufficient for the acquisition of SiPMs, which would need resolutions below 250 ps. There are already TDC architectures which could arrive to such a resolution, but, at the moment, they suffer from a high use of resources. For instance, a cascade of input delays can create a tapped delay line [68], which will further increase the resolution of the TDCs. Hitherto, tapped delays have been implemented using the fast carry logic of the FPGA slices [69] or the FPGA routing resources [70] with high use of resources, which makes them unsuitable for neutrino telescopes. Other architectures of TDCs, with low-resource occupancy and resolutions higher than 250 ps, should be researched. For instance, an improvement of the oversampling architecture can be achieved by increasing the number of phases and the frequency of the master clock. Additionally, a short tapped delay line can be created with input delays, which will have a low resource occupancy, making it ideal for neutrino telescope applications. The average delay in the Kintex-7 family is 39.1 ps, and decreases to only 2.1 ps in the Kintex UltraScale+ Xilinx FPGA [71,72], which would allow both a low resolution and a low non-linearity while continuing to use

minimal FPGA resources. As can be seen, the best architecture, in terms of the tapped delay size and the average delay, is the UltraScale+ family of Xilinx. A scheme of the proposed architecture is presented in Figure 6, in which the architecture already in use in KM3NeT is complemented with a tapped delay line of three delays. Clock frequencies of 500 MHz will give TDC resolutions of 500 ps when using the oversampling technique alone. By using three delays in the tapped delay line, the resolution will increase to 125 ps. Instead, if a tapped delay line of seven delays is used, then the resolution can be further reduced to 75 ps.

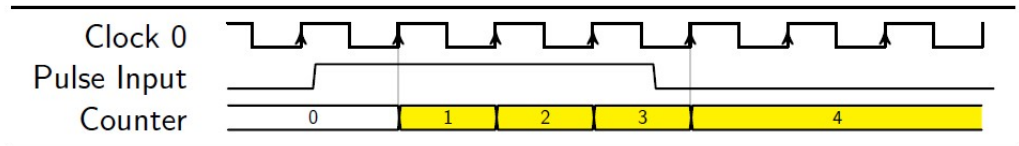
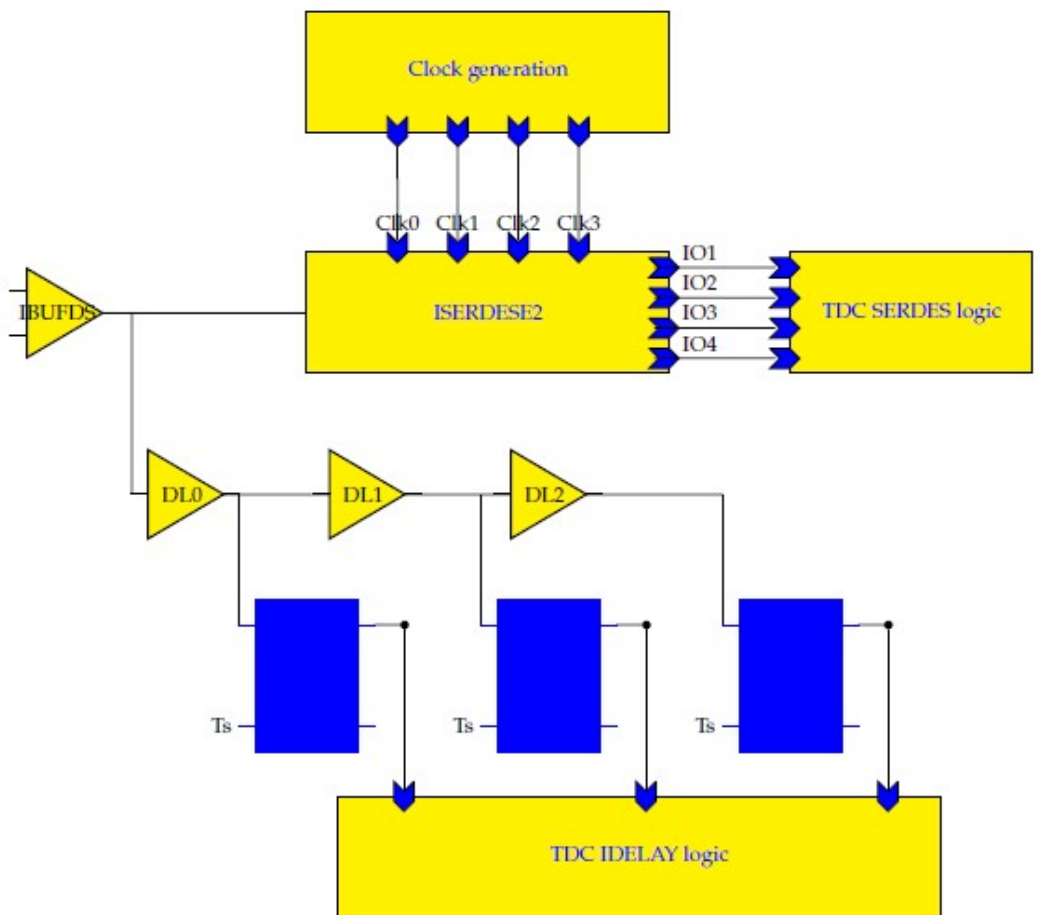


Figure 5. Counter.



**Figure 6.** Oversampling TDC architecture implemented with IOSERDES, expanded with the IDELAY interpolator (three tapped delays). The IOSERDES provide a resolution a quarter of that of the clock frequencies. The resolution is further improved by four by the IDELAY interpolator. It is not shown in the figure, but the latches are triggered by the rising edge of the first phase clock detecting the incoming pulse. The number of IDELAYs can be increased further. By using seven tapped delays of 78 ps ( $2 \times 39.1$  ps), with a clock frequency of 400 MHz, a TDC resolution of 78 ps can be achieved. Note that in the proposed TDC architecture, the tapped delays and the oversampling frequency should match to not add additional non-linearities.

### 5.2. Synchronisation

To complement the resolution of the TDCs, a similar synchronisation level between the acquisition nodes is necessary to perform coincidences between events of different detection nodes. Thus, a synchronisation level between acquisition nodes below 250 ps should be obtained. The FPGA technology selected to implement the TDCs should be able to provide the required level of synchronisation. The White Rabbit protocol has already been used in the KM3NeT FPGA, a Kintex-7 160T from Xilinx. Hitherto, the 16 nm FPGAs, and in particular the Xilinx UltraScale+, provide the best features to implement a low-resource, high-resolution architecture of TDCs. The White Rabbit PTP Core should be embedded into the selected FPGA, and the synchronisation level should be compliant with the sub-nanosecond requirements, and specifically in relation to the determinism of the system. The return of experience of KM3NeT, where a skew of less than 50 ps is obtained [32] (see Figure 7), ensures this possibility.

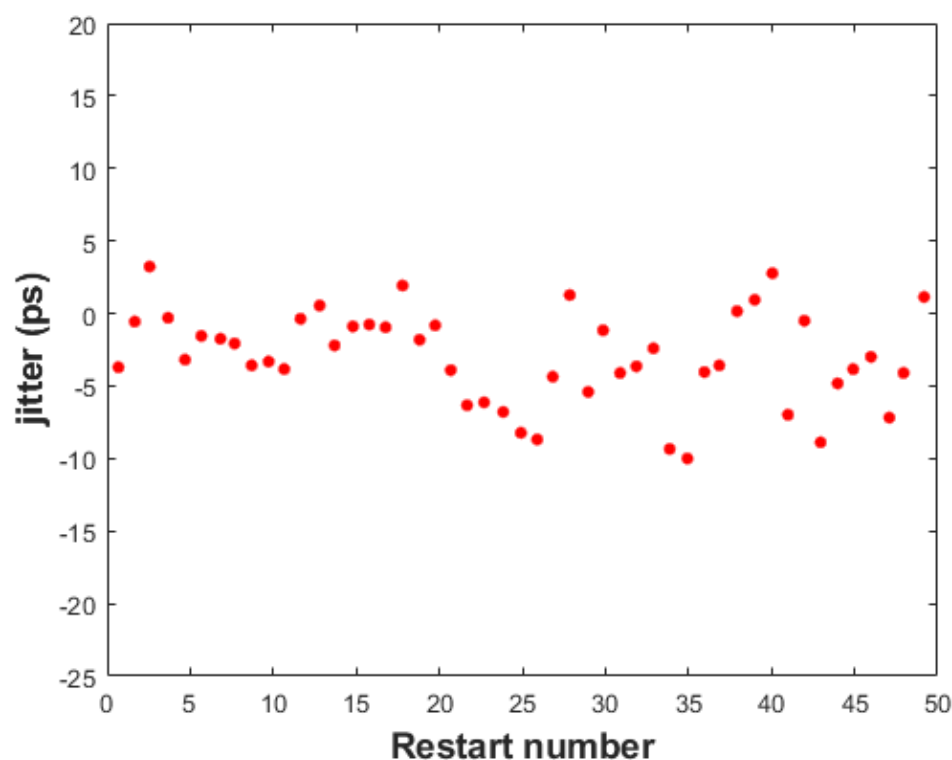


**Figure 7.** Synchronisation achieved in KM3NeT nodes. The skew is measured after several restart cycles of the upgraded acquisition electronics [32]. Each points accumulates 1000 points. The standard deviation obtained is 3.17 ps.

### 5.3. Filtering

While the timing characteristics of SiPMs are improved considerably over those of the PMTs, the DCR of SiPMs presents an additional challenge. The state-of-the-art SiPM DCR, although improved considerably in recent years [51], is around 20–30 kcps/mm<sup>2</sup> at ambient temperature. With these noise rates, a SiPM with a similar detection area as the multi-PMT DOM PMT at seawater temperature will have a dark noise of about 30 Mcps, which cannot be managed by the current readout systems as it will saturate communications. The DCR decreases with temperature, roughly by half every eight degrees [53]. Although the operation temperature of underwater neutrino telescopes would decrease the SiPM DCR by half [73], and by about two orders of magnitude in the case of ice [74], the level of noise is still significant. By increasing the detection threshold over one single photoelectron, a 100-fold reduction in the DCR could be achieved [52], but in this case with the penalty of losing the single-photon event information. Thus, it is peremptory to implement a

noise rejection technique in the acquisition electronics itself. A possible approach would be to reduce the DCR by improving the “all-data-to-shore” scheme by implementing a coincidence filter between channels in the acquisition electronics. The implementation of a coincidence filter in the readout electronics is needed to reduce the high amount of dark noise generated by SiPMs and keep the data to be sent to the central station below the available bandwidth. The time window in which the filtering is performed would be configurable.

The treatment of the acquired data to perform coincidence analyses on the acquisition electronics, and thus effectively reduce the data rate to be transferred to the central station, is, together with the implementation of high-resolution TDCs, one of the critical factors in increasing the angular resolution of neutrino telescopes. The use of FPGA would add flexibility as remote upgrading the filter would be possible, even with the detection nodes already installed.

**6. Possible Architectures**

The use of SiPMs in neutrino telescope detection nodes allows for two DOM architectures beyond the current state of the art.

*6.1. A Hybrid DOM Architecture with PMTs and SiPMs*

The timing performances of a hybrid DOM equipped with additional SiPM channels (see Figure 8) will be improved with respect to the multi PMT-DOM. The effective area will also be increased substantially by the SiPMs, which, together with the increased timing performances, will result in an improvement of the angular resolution. There will be a considerable increase in the data rates of the DOM caused by the DCR of the additional SiPM channels; however, the implementation of a coincidence trigger in the electronics acquisition system of the hybrid DOM will drastically reduce the data rate. This architecture would be appropriate for either ice or water neutrino telescopes.

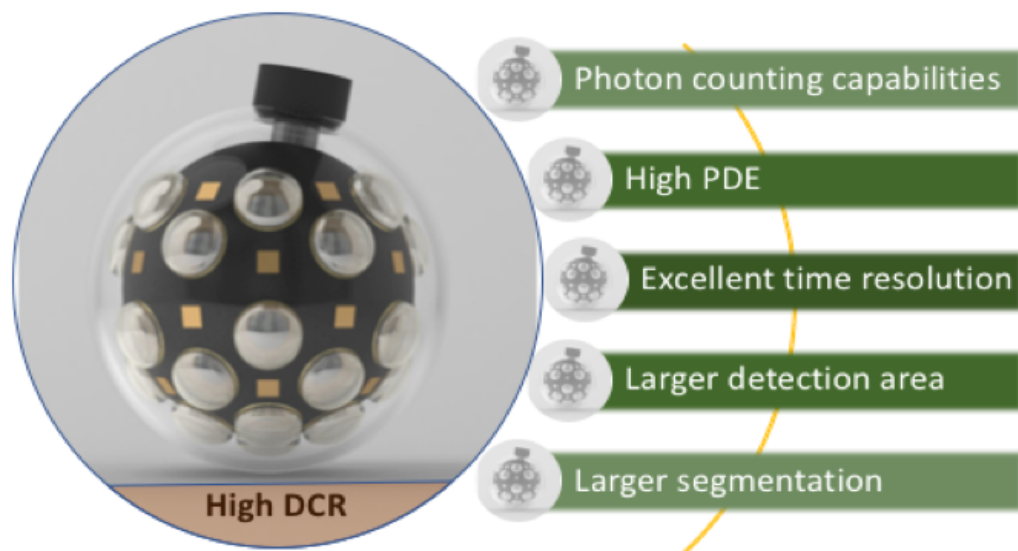


**Figure 8.** Conceptual design of a hybrid DOM with PMTs and SiPMs. Adapted from [15]. SiPM properties, in particular the excellent time resolution, the high PDE, and the possibility of a larger segmentation, represent a challenge for the acquisition electronics.

*6.2. A DOM Architecture Composed Only of SiPMs*

The SiPMs can be organised in panels or detection sections with different areas depending on the position in the DOM surface (i.e., larger areas in the upper part of the DOM and higher segmentation in the DOM bottom hemisphere, which is more relevant to increase the directional sensitivity). This DOM architecture would further improve the angular resolution; however, it would generate a significant amount of noise at ambient

temperatures, so it would be more suitable for ice neutrino telescopes. For water neutrino telescopes, the detection threshold could be increased over the single photoelectron level to achieve a two-order-of-magnitude reduction in the dark noise, but at the cost of losing the single photoelectron information. This configuration could be attractive in a line with hybrid DOMs.

## 7. Conclusions

SiPMs offer a unique opportunity to increase the angular resolution of neutrino telescopes. Although the advantages are clear, SiPMs present two challenges that should be addressed by the acquisition system: an excellent time resolution and an excessively high DCR. The development of TDCs with a sub-250 ps resolution and low resource occupancy, the sub-nanosecond synchronisation provided by the White Rabbit protocol, and the implementation of a coincidence filter in the readout electronics will make possible to use SiPMs as detection sensors, substantially improving the angular resolution of neutrino telescopes and expanding the new window to the extreme Universe that neutrino astronomy has already opened.

**Author Contributions:** Conceptualization, D.R. and D.C.; methodology, D.R. and D.C.; software, D.R.; validation, D.R. and D.C.; formal analysis, D.R. and D.C.; investigation, D.R.; resources, D.R. and D.C.; data curation, D.R. and D.C.; writing—original draft preparation, D.R.; writing—review and editing, D.R. and D.C.; visualization, D.R. and D.C.; supervision, D.R.; project administration, D.R.; funding acquisition, D.R. All authors have read and agreed to the published version of the manuscript.

**Funding:** This research was funded by the Ministerio de Ciencia e Innovación: Programa Estatal para Impulsar la Investigación Científico-Técnica y su Transferencia (refs. PID2021-124591NB-B-C41) (MCIU/FEDER) and Programa de Planes Complementarios I+D+I (refs. ASFAE/2022/023)

**Data Availability Statement:** Data sharing is not applicable to this article.

**Acknowledgments:** The authors acknowledge the financial support of the Ministerio de Ciencia e Innovación: Programa Estatal para Impulsar la Investigación Científico-Técnica y su Transferencia (refs. PID2021-124591NB-B-C41) (MCIU/FEDER), Programa de Planes Complementarios I+D+I (refs. ASFAE/2022/023), Generalitat Valenciana: Prometeo (PROMETEO/2020/019), Grisolia (ref. GRISOLIAP/2021/192) and GenT (refs. CIDEAGENT/2018/034, /2020/049, /2021/23) programs, EU: MSC program (ref. 101025085), Spain.

**Conflicts of Interest:** The authors declare no conflict of interest. The funders had no role in the design of the study; in the collection, analyses, or interpretation of data; in the writing of the manuscript; or in the decision to publish the results.

## References

1. Aartsen, M.G.; Ackermann, M.; Adams, J.; Aguilar, J.A.; Ahlers, M.; Ahrens, M.; Altmann, D.; Andeen, K.; Anderson, T.; Ansseau, I.; et al. The IceCube Neutrino Observatory: Instrumentation and Online Systems. *J. Instrum.* **2017**, *12*, P03012. [[CrossRef](#)]
2. Aartsen, M.G.; Abbasi, R.; Abdou, Y.; Ackermann, M.; Adams, J.; Aguilar, J.A.; Ahlers, M.; Ahrens, M.; Altmann, D.; Auffenberg, J.; et al. Evidence for High-Energy Extraterrestrial Neutrinos at the IceCube Detector. *Science* **2013**, *342*, 1242856. [[CrossRef](#)]
3. Aartsen, M.G.; Ackermann, M.; Adams, J.; Aguilar, J.A.; Ahlers, M.; Ahrens, M.; Altmann, D.; Anderson, T.; Argüelles, C.; Arlen, T.C.; et al. Observation of High-Energy Astrophysical Neutrinos in Three Years of IceCube Data. *Phys. Rev. Lett.* **2014**, *113*, 101101. [[CrossRef](#)]
4. Aartsen, M.G.; Ackermann, M.; Adams, J.; Aguilar, J.A.; Ahlers, M.; Ahrens, M.; Altmann, D.; Andeen, K.; Anderson, T.; Ansseau, I.; et al. Multimessenger observations of a flaring blazar coincident with high-energy neutrino IceCube-170922A. *Science* **2018**, *361*, eaat1378. [[CrossRef](#)]
5. Aartsen, M.G.; Ackermann, M.; Adams, J.; Aguilar, J.A.; Ahlers, M.; Ahrens, M.; Alispach, C.; Andeen, K.; Anderson, T.; Ansseau, I.; et al. Time-Integrated Neutrino Source Searches with 10 Years of IceCube Data. *Phys. Rev. Lett.* **2020**, *124*, 051103. [[CrossRef](#)]
6. Abbasi, R.; Ackermann, M.; Adams, J.; Aguilar, J.A.; Ahlers, M.; Ahrens, M.; Alameddine, J.M.; Alispach, C.; Alves, A.A.; Amin, N.M.; et al. Evidence for neutrino emission from the nearby active galaxy NGC 1068. *Science* **2022**, *378*, 538–543. [[CrossRef](#)] [[PubMed](#)]
7. Ageron, M.; Aguilar, J.A.; Al Samarai, I.; Albert, A.; Ameli, F.; André, M.; Anghinolfi, M.; Anton, G.; Anvar, S.; Ardid, M.; et al. ANTARES: The first undersea neutrino telescope. *Nucl. Instrum. Meth. A* **2011**, *656*, 11–38. [[CrossRef](#)]

8. Adrian-Martinez, S.; Ageron, M.; Aharonian, F.; Aiello, S.; Albert, A.; Ameli, F.; Anassontzis, E.; André, M.; Androulakis, G.; Anghinolfi, M.; et al. Letter of intent for KM3NeT 2.0. *J. Phys. G* **2016**, *43*, 084001. [[CrossRef](#)]
9. Agostini, M.; Böhmer, M.; Bosma, J.; Clark, K.; Danninger, M.; Fruck, C.; Gernhäuser, R.; Gärtner, A.; Grant, D.; Henningsen, F.; et al. The Pacific Ocean Neutrino Experiment. *Nat. Astron.* **2020**, *4*, 913–915. [[CrossRef](#)]
10. Ye, Z.P.; Hu, F.; Tian, W.; Chang, Q.C.; Chang, Y.L.; Cheng, Z.S.; Gao, J.; Ge, T.; Gong, G.H.; Guo, J.; et al. Proposal for a neutrino telescope in South China Sea. *arXiv* **2022**, arXiv:2207.04519.
11. Fang, K.; Kotera, K.; Miller, M.C.; Murase, K.; Oikonomou, F. Identifying Ultrahigh-Energy Cosmic-Ray Accelerators with Future Ultrahigh-Energy Neutrino Detectors. *J. Cosmol. Astropart. Phys.* **2016**, *12*, 17. [[CrossRef](#)]
12. Otte, A.N. SiPM's a very brief review. In Proceedings of the International Conference on New Photo-Detectors 2016, Moscow, Russia, 6–9 July 2015; p. 1. [[CrossRef](#)]
13. Acerbi, F.; Gundacker, S. Understanding and simulating SiPMs. *Nucl. Instrum. Meth. A* **2019**, *926*, 16–35. [[CrossRef](#)]
14. Saveliev, V. Silicon Photomultiplier—New Era of Photon Detection. In *Advances in Optical and Photonic Devices*; Kim, K.Y., Ed.; IntechOpen: Rijeka, Croatia, 2010; Chapter 14. [[CrossRef](#)]
15. Hu, F.; Li, Z.; Xu, D. Exploring a PMT+SiPM hybrid optical module for next generation neutrino telescopes. In Proceedings of the 37th International Cosmic Ray Conference (ICRC2021), Berlin, Germany, 18 March 2022. [[CrossRef](#)]
16. Norris, R.P. Discovering the Unexpected in Astronomical Survey Data. *Publ. Astron. Soc. Aust.* **2017**, *34*, e007. [[CrossRef](#)]
17. Markov, M.A. On high energy neutrino physics. In Proceedings of the 10th International Conference on High Energy Physics, Rochester, NY, USA, 25 August–1 September 1960; pp. 578–581.
18. Hazen, E.S.; Alexander, C.M.; Anderson, E.W.; Aoki, T.; Berns, H.G.; Berson, U.; Bosetti, P.C.; Bolesta, P.E.; Boynton, P.E. The DUMAND-II digitizer. In Proceedings of the 23rd International Cosmic Ray Conference, Calgary, AB, Canada, 19–30 July 1993.
19. Aiello, S.; Albert, A.; Alves Garre, S.; Aly, Z.; Ameli, F.; André, M.; Androulakis, G.; Anghinolfi, M.; Anguita, M.; Gisela, A.; et al. Architecture and performance of the KM3NeT front-end firmware. *J. Astron. Telesc. Instrum. Syst.* **2021**, *7*, 016001. [[CrossRef](#)]
20. Ameli, F.; Aiello, S.; Aloisio, A.; Amore, I.; Anghinolfi, M.; Anzalone, A.; Avanzini, C.; Barbarino, G.; Barbarito, E.; Battaglieri, M.; et al. The Data Acquisition and Transport Design for NEMO Phase 1. *IEEE Trans. Nucl. Sci.* **2008**, *55*, 233–240. [[CrossRef](#)]
21. Klein, S.R. IceCube: A Cubic Kilometer Radiation Detector. *IEEE Trans. Nucl. Sci.* **2009**, *56*, 1141–1147. [[CrossRef](#)]
22. Andres, E.; Askebjerg, P.; Barwick, S.W.; Bay, R.; Bergström, L.; Biron, A.; Booth, J.; Bouchta, A.; Carius, S.; Carlson, M.; et al. The AMANDA neutrino telescope: Principle of operation and first results. *Astropart. Phys.* **2000**, *13*, 1–20. [[CrossRef](#)]
23. Aguilar, J.A.; Al Samarai, I.; Albert, A.; Anghinolfi, M.; Anton, G.; Anvar, S.; Ardid, M.; Assis Jesus, A.C.; Astraatmadja, T.; Aubert, J.J.; et al. Performance of the front-end electronics of the ANTARES neutrino telescope. *Nucl. Instrum. Meth. A* **2010**, *622*, 59–73. [[CrossRef](#)]
24. Aiello, S.; Albert, A.; Alshamsi, M.; Garre, S.A.; Aly, Z.; Ambrosone, A.; Ameli, F.; Andre, M.; Androulakis, G.; Anghinolfi, M.; et al. The KM3NeT multi-PMT optical module. *J. Instrum.* **2022**, *17*, P07038. [[CrossRef](#)]
25. van Eeden, T.; Seneca, J.; Heijboer, A. High-energy reconstruction for single and double cascades using the KM3NeT detector. In Proceedings of the 37th International Cosmic Ray Conference, Berlin, Germany, 12–23 July 2021. [[CrossRef](#)]
26. Bouwhuis, M. Time synchronization and time calibration in KM3NeT. In Proceedings of the 34th International Cosmic Ray Conference, The Hague, The Netherlands, 30 July–6 August 2015. [[CrossRef](#)]
27. Coniglione, R.; Creusot, A.; Di Palma, I.; Guderian, D.; Hofestädt, J.; Riccobene, G.; Sánchez Losa, A. KM3NeT Time Calibration. In Proceedings of the 36th International Cosmic Ray Conference, Madison, WI, USA, 24 July–1 August 2019. [[CrossRef](#)]
28. Jansweijer, P.P.M.; Peek, H.Z.; De Wolf, E. White Rabbit: Sub-nanosecond timing over Ethernet. *Nucl. Instrum. Meth. A* **2013**, *725*, 187–190. [[CrossRef](#)]
29. Serrano, J.; Alvarez, P.; Cattin, M.; Garcia Cota, E.; Lewis, J.; Moreira, P.; Wlostowski, T.; Gaderer, G.; Loschmidt, P.; Dedic, J.; et al. White Rabbit Project. In Proceedings of the ICALEPCS2009, Kobe, Japan, 12–16 October 2009; pp. 93–95.
30. Lipinski, M.; Wlostowski, T.; Serrano, J.; Alvarez, P. White rabbit: A PTP application for robust sub-nanosecond synchronization. In Proceedings of the 2011 IEEE International Symposium on Precision Clock Synchronization for Measurement, Control and Communication, Munich, Germany, 12–16 September 2011; pp. 25–30.
31. Calvo, D.; Real, D.; Carrió, F. Sub-nanosecond synchronization node for high-energy astrophysics: The KM3NeT White Rabbit Node. *Nucl. Instrum. Meth. A* **2020**, *958*, 162777. [[CrossRef](#)]
32. Real, D.; Bozza, C.; Calvo, D.; Musico, P.; Jansweijer, P.; Colonges, S.; van Beveren, V.; Versari, F.; Chiarusi, T.; Carrió, F.; et al. KM3NeT acquisition: The new version of the Central Logic Board and its related Power Board, with highlights and evolution of the Control Unit. *J. Instrum.* **2020**, *15*, C03024. [[CrossRef](#)]
33. Aiello, S.; Albert, A.; Alshamsi, M.; Garre, S.A.; Aly, Z.; Ambrosone, A.; Ameli, F.; Andre, M.; Androulakis, G.; Anghinolfi, M.; et al. Nanobeacon: A time calibration device for the KM3NeT neutrino telescope. *Nucl. Instrum. Meth. A* **2022**, *1040*, 167132. [[CrossRef](#)]
34. Ageron, M.; Aguilar, J.A.; Albert, A.; Ameli, F.; Anghinolfi, M.; Anton, G.; Anvar, S.; Ardellier-Desages, E.; Aslaniedes, E.; Aubert, J.J.; et al. The ANTARES Optical Beacon System. *Nucl. Instrum. Meth. A* **2007**, *578*, 498–509. [[CrossRef](#)]
35. Anvar, S. Data acquisition architecture studies for the KM3NeT deep sea neutrino telescope. In Proceedings of the 2008 IEEE Nuclear Science Symposium and Medical Imaging Conference and 16th International Workshop on Room-Temperature Semiconductor X-Ray and Gamma-Ray Detectors, Dresden, Germany, 19–25 October 2008; pp. 3558–3561. [[CrossRef](#)]

36. Biagi, S.; Chiarusi, T.; Piattelli, P.; Real, D. The data acquisition system of the KM3NeT detector. In Proceedings of the 34th International Cosmic Ray Conference, The Hague, The Netherlands, 30 July–6 August 2015. [CrossRef]
37. Pellegrino, C. The Trigger and Data Acquisition System (TriDAS) of the KM3NeT experiment. *Nuovo Cim. C* **2016**, *39*, 250. [CrossRef]
38. Ishihara, A. The IceCube Upgrade—Design and Science Goals. In Proceedings of the 36th International Cosmic Ray Conference, Madison, WI, USA, 24 July–1 August 2019; p. 1031. [CrossRef]
39. Classen, L.; Kossatz, M.; Kretzschmann, A.; Lindner, S.; Shuklin, D. The mDOM—A multi-PMT digital optical module for the IceCube-Gen2 neutrino telescope. In Proceedings of the 35th International Cosmic Ray Conference, Busan, Republic of Korea, 10–20 July 2017. [CrossRef]
40. Classen, L.; Dorn, C.; Kappes, A.; Karg, T.; Kossatz, M.; Kretzschmann, A.; Ortjohann, H.W.; Reubelt, J.; Sulanke, K.H.; Weigel, R. A multi-PMT Optical Module for the IceCube Upgrade. In Proceedings of the 36th International Cosmic Ray Conference, Madison, WI, USA, 24 July–1 August 2019. [CrossRef]
41. Anderson, T.; Classen, L.; Fienberg, A.T.; Mechbal, S.; Scheneider, J.; Sulanke, K.H.; Unland Elorrieta, M.A.; Wendt, W.; et al. Design and performance of the multi-PMT optical module for IceCube Upgrade. In Proceedings of the 37th International Cosmic Ray Conference, Berlin, Germany, 12–23 July 2021. [CrossRef]
42. Aiello, S.; Ameli, F.; André, M.; Androulakis, G.; Anghinolfi, M.; Anton, G.; Aublin, J.; Bagatelas, C.; Barbarino, G.; et al. KM3NeT front-end and readout electronics system: Hardware, firmware and software. *J. Astron. Telesc. Instrum. Syst.* **2019**, *5*, 046001. [CrossRef]
43. KETEK. Datasheet SiPM PM3325-WB-D0. Available online: <https://www.ketek.net/wp-content/uploads/2018/12/KETEK-PM3325-WB-D0-Datasheet.pdf> (accessed on 25 January 2023).
44. Acerbi, F.; Ferri, A.; Gola, A.; Cazzanelli, M.; Pavesi, L.; Zorzi, N.; Piemonte, C. Characterization of Single-Photon Time Resolution: From Single SPAD to Silicon Photomultiplier. *IEEE Trans. Nucl. Sci.* **2014**, *61*, 2678–2686. [CrossRef]
45. Ghassemi, A.; Sato, K.; Kobayashi, K. MMPC. 2008. Available online: [https://www.hamamatsu.com/content/dam/hamamatsu-photonics/sites/documents/99\\_SALES\\_LIBRARY/ssd/mppc\\_kapd9005e.pdf#page=27](https://www.hamamatsu.com/content/dam/hamamatsu-photonics/sites/documents/99_SALES_LIBRARY/ssd/mppc_kapd9005e.pdf#page=27) (accessed on 25 January 2023).
46. Donati, S. Avalanche Photodiode, SPAD, and SiPM. In *Photodetectors: Devices, Circuits and Applications*; IEEE: Piscataway, NJ, USA, 2021; pp. 175–220. [CrossRef]
47. Sun, Y.; Maricic, J. SiPMs characterization and selection for the DUNE far detector photon detection system. *J. Instrum.* **2016**, *11*, C01078. [CrossRef]
48. Yebras, J.; Antoranz, P.; Miranda, J. Single Photon Counting with Silicon Photomultipliers, shortening systems and incoherent illumination. *J. Eur. Opt. Soc. Rapid Publ.* **2012**, *7*, 12014. [CrossRef]
49. Gola, A.; Acerbi, F.; Capasso, M.; Marcante, M.; Mazzi, A.; Paternoster, G.; Piemonte, C.; Regazzoni, V.; Zorzi, N. NUV-Sensitive Silicon Photomultiplier Technologies Developed at Fondazione Bruno Kessler. *Sensors* **2019**, *19*, 308. [CrossRef]
50. Aiello, S.; Akrame, S.E.; Ameli, F.; Anassontzis, E.G.; Andre, M.; Androulakis, G.; Anghinolfi, M.; Anton, G.; Ardid, M.; Aublin, J.; et al. Characterisation of the Hamamatsu photomultipliers for the KM3NeT Neutrino Telescope. *J. Instrum.* **2018**, *13*, P05035. [CrossRef]
51. Acerbi, A.; Paternoster, G.; Gola, A. SiPM Overview: Status and Trends. Communication to the International Workshop on New Photon-Detectors. 2018. Available online: [https://indico.ipmu.jp/event/166/contributions/2809/attachments/2133/2596/FBK\\_Acerbi\\_-\\_SiPM\\_overview\\_v5a.pdf](https://indico.ipmu.jp/event/166/contributions/2809/attachments/2133/2596/FBK_Acerbi_-_SiPM_overview_v5a.pdf) (accessed on 25 January 2023).
52. Korpar, S. SiPMs-Technologies and Timing. FT4. 2019. Available online: <https://indico.cern.ch/event/999817/contributions/4253051/attachments/2240249/3798094/TF4-Korpar.pdf> (accessed on 25 January 2023).
53. Ootani, W. Silicon Photomultiplier (SiPM) Status and Perspectives. 2015. Available online: [https://indico.cern.ch/event/392833/contributions/1829473/attachments/785875/1077253/SiPMReview\\_OotaniRD51.pdf](https://indico.cern.ch/event/392833/contributions/1829473/attachments/785875/1077253/SiPMReview_OotaniRD51.pdf) (accessed on 25 January 2023).
54. Adrian-Martinez, S.; Ageron, M.; Aguilar, J.A.; Aharonian, F.; Aiello, S.; Albert, A.; Alexandri, M.; Ameli, F.; Anassontzis, E.; Androulakis, G.; et al. Expansion cone for the 3-inch PMTs of the KM3NeT optical modules. *J. Instrum.* **2013**, *8*, T03006. [CrossRef]
55. Pavia, J.; Wolf, M.; Charbon, E. Measurement and modeling of microlenses fabricated on single-photon avalanche diode arrays for fill factor recovery. *Opt. Express* **2014**, *22*, 4202–4213. [CrossRef]
56. Engelmann, E. *Dark Count Rate of Silicon Photomultipliers: Metrological Characterization and Suppression*; Cuvillier Verlag: Gottingen, Germany, 2018.
57. Hamamatsu. SiPM S13360 Series Datasheet. 2022. Available online: [https://www.hamamatsu.com/content/dam/hamamatsu-photonics/sites/documents/99\\_SALES\\_LIBRARY/ssd/s13360\\_series\\_kapd1052e.pdf](https://www.hamamatsu.com/content/dam/hamamatsu-photonics/sites/documents/99_SALES_LIBRARY/ssd/s13360_series_kapd1052e.pdf) (accessed on 25 January 2023).
58. OnSemi. SiPM C Series Datasheet. 2022. Available online: <https://www.onsemi.com/pdf/datasheet/microc-series-d.pdf> (accessed on 25 January 2023).
59. Grupen, C.; Shwartz, B. *Particle Detectors*, 2nd ed.; Cambridge Monographs on Particle Physics, Nuclear Physics and Cosmology; Cambridge University Press: Cambridge, UK, 2008. [CrossRef]
60. Kalisz, J. Review of methods for time interval measurements with picosecond resolution. *Metrol. Metrol.* **2004**, *41*, 17–32. [CrossRef]
61. Xilinx. Kintex Ultrascale Series FPGAs Data Sheet. 2020. Available online: <https://docs.xilinx.com/v/u/en-US/ds892-kintex-ultrascale-data-sheet> (accessed on 24 June 2023).
62. Nutt, R. Digital Time Intervalometer. *Rev. Sci. Instrum.* **1968**, *39*, 1342–1345. [CrossRef]

63. Wu, J.; Hansen, S.; Shi, Z. ADC and TDC implemented using FPGA. In Proceedings of the 2007 IEEE Nuclear Science Symposium and Medical Imaging Conference, Honolulu, HI, USA, 26 October–3 November 2007; Volume 1, pp. 281–286. [CrossRef]
64. Yuan, Q.; Zhang, B.; Wu, J.; Zaghoul, M. A high resolution time-to-digital converter on FPGA for Time-Correlated Single Photon Counting. In Proceedings of the 2012 IEEE 55th International Midwest Symposium on Circuits and Systems (MWSCAS), Boise, ID, USA, 5–8 August 2012; pp. 900–903. [CrossRef]
65. Spencer, D.; Cole, J.; Drigert, M.; Aryaiejad, R. A high-resolution, multi-stop, time-to-digital converter for nuclear time-of-flight measurements. *Nucl. Instrum. Methods Phys. Res. Sect. A Accel. Spectrometers Detect. Assoc. Equip.* **2006**, *556*, 291–295. [CrossRef]
66. Balla, A.; Mario Beretta, M.; Ciambrone, P.; Gatta, M.; Gonnella, F.; Iafolla, L.; Mascolo, M.; Messi, R.; Moricciani, D.; Riandino, D. The characterization and application of a low resource FPGA-based time to digital converter. *Nucl. Instrum. Methods Phys. Res. Sect. A Accel. Spectrometers Detect. Assoc. Equip.* **2014**, *739*, 75–82. [CrossRef]
67. Calvo, D.; Real, D. High resolution time to digital converter for the KM3NeT neutrino telescope. *J. Instrum.* **2015**, *10*, C01015. [CrossRef]
68. Jayasinghe, D.; Ignjatovic, A.; Parameswaran, S. UCloD: Small Clock Delays to Mitigate Remote Power Analysis Attacks. *IEEE Access* **2021**, *9*, 108411–108425. [CrossRef]
69. Qi, J.; Gong, H.; Liu, Y. On-Chip Real-Time Correction for a 20-ps Wave Union Time-To-Digital Converter (TDC) in a Field-Programmable Gate Array (FPGA). *IEEE Trans. Nucl. Sci.* **2012**, *59*, 1605–1610. [CrossRef]
70. Wang, H.; Zhang, M.; Yao, Q. A new realization of time-to-digital converters based on FPGA internal routing resources. *IEEE Trans. Ultrason. Ferroelectr. Freq. Control* **2013**, *60*, 1787–1795. [CrossRef] [PubMed]
71. Xilinx. Kintex7 Series FPGAs Data Sheet. 2020. Available online: [https://docs.xilinx.com/v/u/en-US/ds182\\_Kintex\\_7\\_Data\\_Sheet](https://docs.xilinx.com/v/u/en-US/ds182_Kintex_7_Data_Sheet) (accessed on 24 June 2023).
72. Xilinx. XCKU5P Ultrascale+ Series FPGAs Data Sheet. Available online: <https://datasheet.octopart.com/XCKU5P-2FFVB676I-Xilinx-datasheet-94062434.pdf> (accessed on 24 June 2023).
73. Bagley, P.; Craig, J.; Holford, A.; Jamieson, A.; Niedzielski, T.; Priede, I.G.; de Bell, M.; Koopstra, J.; Lim, G.; de Wolf, E.; et al. KM3NeT: Technical Design Report for a Deep-Sea Research Infrastructure in the Mediterranean Sea Incorporating a Very Large Volume Neutrino Telescope. 2009. Available online: <https://www.roma1.infn.it/people/capone/KM3NeT/KM3NeT-TDR.pdf> (accessed 24 June 2023).
74. Nagornov, O.; Bay, R.; Chirkin, D.; He, Y.; Miocinovic, P.; Richards, A.; Woschnagg, K.; Koci, B.; Zagorodnov, V.; Pricet, P.B.; et al. Temperature profile for glacial ice at the South Pole: Implications for life in a nearby subglacial lake. *Proc. Natl. Acad. Sci. USA* **2002**, *99*, 7844–7847. [CrossRef]

**Disclaimer/Publisher’s Note:** The statements, opinions and data contained in all publications are solely those of the individual author(s) and contributor(s) and not of MDPI and/or the editor(s). MDPI and/or the editor(s) disclaim responsibility for any injury to people or property resulting from any ideas, methods, instructions or products referred to in the content.